Electronic Supplementary Material (ESI) for Journal of Materials Chemistry A.

17% efficient printable mesoscopic PIN metal oxides framework perovskite solar cells using cesium-containing triple cation-perovskite

Shungshuang Liu,[a] Wenchao Huang,[b] Peizhe Liao,[a] Nuttapol Pootrakulchote,[c] Hao Li,[a] Jianfeng Lu, [d] Junpeng Li, [e] Feihong Huang, [a] Xuxia Shai, [a] Xiaojuan Zhao, [a] Yan Shen, [a] Yibing Cheng, [a] Mingkui Wang [a*]

[a] Wuhan National Laboratory for Optoelectronics, Huazhong University of Science and Technology, Luoyu Road 1037, Wuhan 430074, P. R. China.

[b] Department of Materials Science and Engineering, University of California, Los Angeles, California 90095, USA

[c] Department of Chemical Technology, Faculty of Science, Chulalongkorn University Phayathai Road, Pathumwan Bangkok 10330, Thailand

[d] Department of Materials Engineering, Monash University, Victoria 3800, Australia

[e] Kunming Institute of Precious Metals, Kunming 650106, P. R. China.

Experimental Section

Synthesis of MAI and FAI: In brief, MAI was synthesized by adding 15 mL methylamine (40% in methanol, Aladdin) and 16.15 mL hydroiodic acid (57% in water, Aldrich) at 0 °C with stirring for 2 hours. To precipitate MAI, the following step was used to remove the solvents by rotary evaporation and washed the products several times with diethyl ether. White crystals were obtained after drying in vacuum for 3 days. FAI was prepared by reacting 0.1 mol FA solution with 0.09 mol aqueous HI in a round bottom flask for 2 h. The resulting FAI was collected using rotary evaporator at 50 °C for 1 h. Light yellow color FAI was washed with diethyl ether three times and dried in vacuum for 12 h. [1, 2]

Preparation of carbon, Al_2O_3, and TiO_2 pastes: 0.588 g ZrO_2 (50 nm, Aladdin), 4 g graphite (8000 mesh) and 1 g carbon black (EC300) were added. This solution was treated with an ultrasonic probe for 5 min, followed by magnetic stirring for 10 min, and those processes were repeated three times. The mixture was dispersed in ethyl alcohol, in which 17.6 mL terpilenol was added. The mixture was then treated by an ultrasonic probe for 5 min, followed by magnetic stirring for 10 min, and ball-milling for 16 h. 2.94 g ethyl cellulose was added to the mixture. In the last step, the ethyl alcohol was removed with rotary evaporation. Al_2O_3 (20 nm γ-Al_2O_3 nanoparticles, Aladdin) paste was prepared by mixing 3g of Al_2O_3 nano powder in 80 mL ethanol and subsequently adding with 15 g 10 wt% ethyl cellulose (in EtOH) and10g terpineol.

The prepared process of NiO is similar to that of Al_2O_3 paste. The TiO_2 paste (18 nm) was purchased from Dyesol Corporation, and diluted with ethanol by a ratio of 1:2.[3]

Characterization: The film thickness was measured with profile-meter (Veeco Dektak 150). The cross section of the sample was characterized with a field-emission scanning electron microscope (FE-SEM). Energy dispersive spectrometer (EDS) images were obtained using FEI Nova Nano-SEM 450. For the nanosecond transient absorption spectroscopy, about 50 μJ of pulse energy as the fundamental output from a Ti: Sapphire femtosecond regenerative amplifier (800 nm, 35 fs FWHM, 1 kHz, Newport Spectra-Physics) was used to generate pump and probe beams. By introducing the fundamental beams into an optical parametric amplifier (Light Conversion Ltd), we could select a certain wavelength from the tunable output as the pump pulses, whereas light continuum probe pulses were obtained by focusing the fundamental beams onto a sapphire plate (contained in LP920, Edinburgh Instruments). The transmitted probe light from the samples was collected and focused on the broadband VIS-NIR detector for recording the time-resolved excitation induced difference spectrum (ΔOD). The photocurrent-voltage (J-V) characteristics of solar cells were measured by recording the current through Keithley 2400 digital source meter. A Xenon light source solar simulator (450W, Oriel, model 9119) with AM 1.5G filter (Oriel, model 91192) was used to give an irradiance of 100 mW cm^{-2} at the surface of the solar cells. The solar-cell parameters were obtained using an AM 1.5 G solar simulator with an irradiation intensity of 100 mW

cm^{-2}. The lamp was calibrated with an Newport-calibrated silicon reference cell (ORIEL). The devices were tested using a metal mask with an area of 0.129 cm^2. For the EQE measurements, a white-light bias (10% sunlight intensity) was applied onto the sample during the EQE measurements with the DC model. The electronic impedance measurements (IS) were performed using the PGSTAT302N frequency analyzer from Autolab (The Netherlands) together with the Frequency Response Analyzer to give voltage modulation under the giving range of frequency. The working electrode was linked with positive electrode, while the counter electrode was linked with negative electrode. The Z-view software (v2.8b) was used to analyze the impedance data. The photovoltage/photocurrent transient decay (TPD) measurement was carried out to obtain the electron diffusion length (HuaMing, model III). A white light bias on the device sample was generated from an array of diodes. A ring of red laser pulse was controlled by a fast solid-state switch. Transient decays were measured at different white light intensities via tuning the voltage applied to the bias diodes. The voltage output was recorded on an oscilloscope directly connected with the cells.

The Goldschmidt tolerance factor is calculated from the ionic radius of the atoms using the following expression:

$$t = \frac{(r_A + r_X)}{\sqrt{2}(r_B + r_X)}$$

where r_A and r_B are the ionic radius of the A and B site cations respectively. r_X is the ionic radius of the anion. The tolerance factor can be an effectively indicator to estimate whether the A site cation can fit within the cavities in the BX_3 framework. A tolerance factor of 1 indicates a perfect fit; in the range $0.8 \leq t \leq 1$ perovskites generally do form. But in the range of $0.8 \leq t \leq 0.9$, the perovskite structure may be distorted due to tilting of the BX_6 octahedral and lowering of the symmetry while the cubic perovskite structure is formed in the range of $0.8 < t \leq 1$. If $t > 1$, this indicates the A site cation is too large and generally precludes formation of a perovskite, and if $t < 0.8$, the A cation is too small, again often leading to alternative structures. [4]

The photovoltaic experiment was performed to evaluate the influence of different ratio of FA/MA and $PbI_2/PbBr_2$ ratio in precursor solution on devices performance. Figure S1a presents the J-V (reverse scan) and curves for devices with different FA/MA ratio under standard AM 1.5G illumination at 100 mW cm^{-2}. All devices were fabricated by keeping the TiO_2/Al_2O_3/NiO/carbon film at constant thickness (TiO_2 ~460 nm, Al_2O_3~450 nm, NiO ~800 nm and carbon ~10 µm). The PCE of device is 7.75%, 9.73%, 9.23%, 8.96% with MA/FA ratio is 4:1, 3:2, 2:3, 1:4, respectively. The detailed photovoltaics parameters are listed in Table S1, which can be evaluated the best MA/FA ratio is 3:2. Then, as shown in Figure S1b and Table S2, we evaluated the PbI_2 and $PbBr_2$ ratio in precursor solution. The PCE of device is 8.35%, 10.21%, 8.71%, 5.56% with the ratio of PbI_2 and $PbBr_2$ is 1:0, 9:1, 4:1, 3:2, respectively when MA/FA ratio was 3:2. We can find that the best PbI_2 and $PbBr_2$ ratio is 9:1.

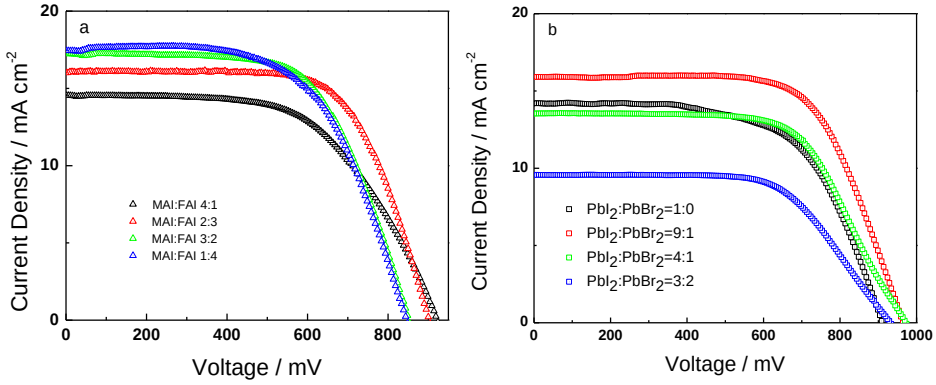

Figure S1. J-V curves of various perovskite solar cell devices under standard AM 1.5G illumination at 100 mW cm^{-2} for devices (a)with MAI:FAI= 4:1, 2:3, 3:2, 1:4, respectively (b) with PbI_2:$PbBr_2$=1:0, 9:1, 4:1, 3:2, respectively.

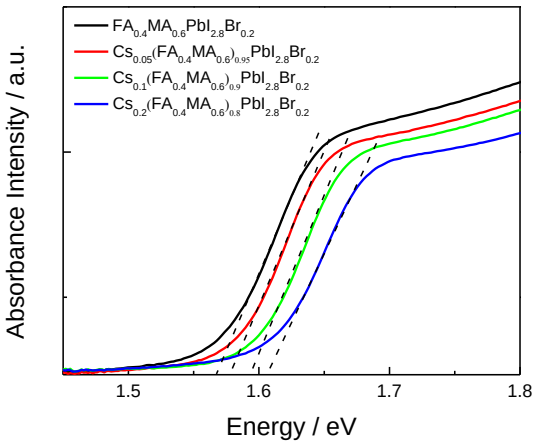

Figure S2. The UV-Vis absorption of $Cs_x(FA_{0.4}MA_{0.6})_{1-x}PbI_{2.8}Br_{0.2}$(x=0, 0.05, 0.1, 0.2).

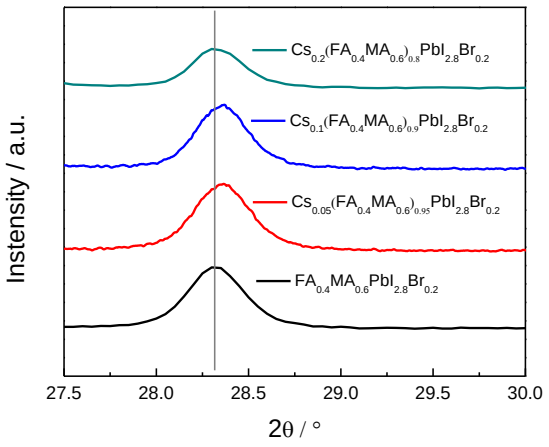

Figure S3. The angle peaks diffraction variation as a function of x of Cs component between 27.5° and 30.0°.

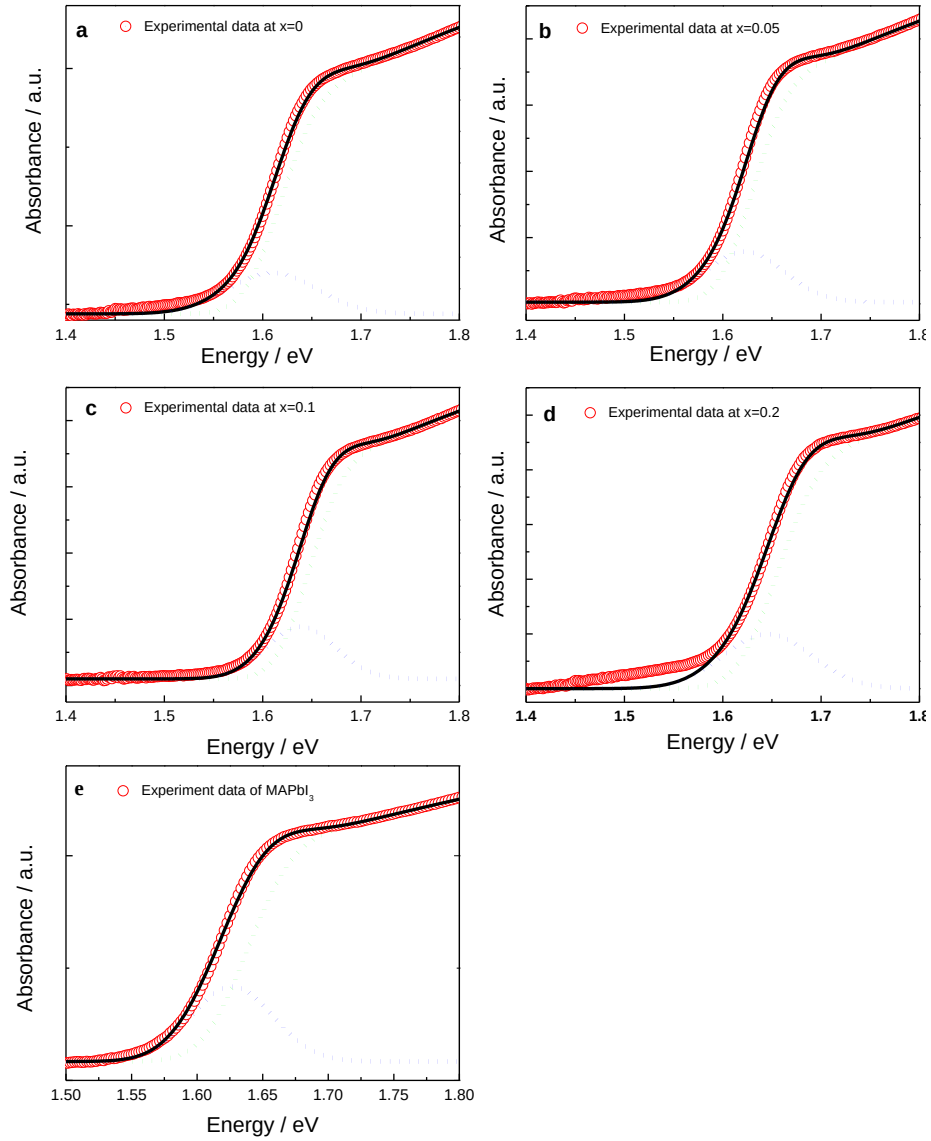

Figure S4. The absorption spectra (red circles) of $Cs_x(FA_{0.4}MA_{0.6})_{1-x}PbI_{2.8}Br_{0.2}$ at a) x=0, b) x=0.05, c)x=0.1, d)x=0.2 and e) $MAPbI_3$ obtained from UV-vis spectra measurement. The black-line is the modeled absorption coefficient with continuum (green-dash line) and excitonic (blue-dash line) components.

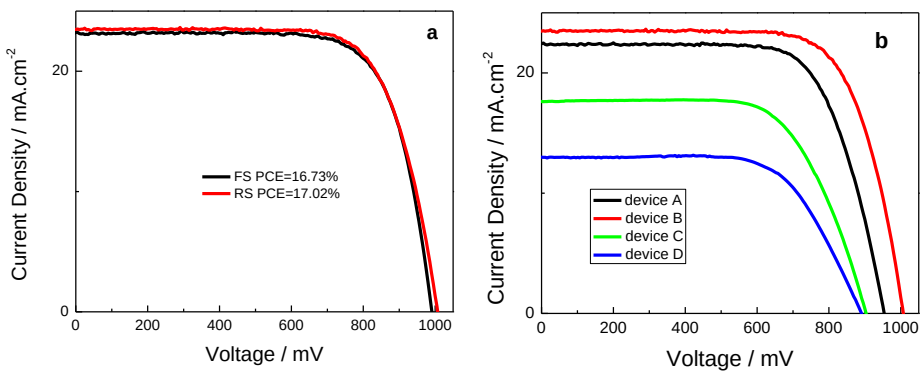

Figure S5. J-V curves of various perovskite solar cell devices under standard AM 1.5G illumination at 100 mW cm^{-2} for (a)device B with forward and reverse scan (b)device A with $FA_{0.4}MA_{0.6}PbI_{2.8}Br_{0.2}$, devices B with $Cs_{0.05}(FA_{0.4}MA_{0.6})_{0.95}PbI_{2.8}Br_{0.2}$, device C with $Cs_{0.1}(FA_{0.4}MA_{0.6})_{0.9}PbI_{2.8}Br_{0.2}$, and device D with $Cs_{0.2}(FA_{0.4}MA_{0.6})_{0.8}PbI_{2.8}Br_{0.2}$ absorbed layer, respectively.

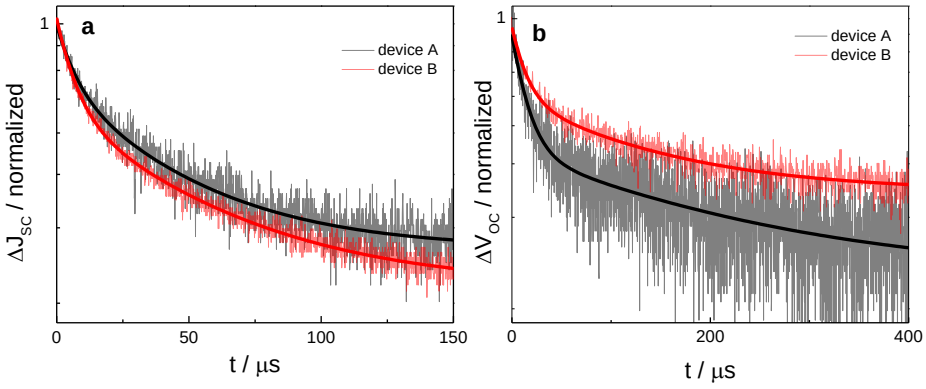

Figure S6. (a)Transient photocurrent decay curves of device A and device B under short-circuit conditions. The solid lines are fitting curves with a bi-exponential equation. (b) Transient photovoltage decay curves of device A and device B under open-circuit conditions. The solid lines are fitting curves with a bi-exponential equation.

Electronic IS measurement was performed to investigate the internal electrical properties of these devices. Figure S8a and S8b show the Nyquist plots and the corresponding Bode phase plots in the frequency range from 2 MHz to 10 mHz for device B under illumination (100% intensity, LED light source) at a bias of 0.75 V. The resulting frequency analysis shows three separated semicircles in the Nyquist diagram (Figure S8a) correlating with three peaks in the Bode plot (Figure S8b). The detailed explanation about three separated semicircles has been reported in our previous works. [5, 6] We have fitted the IS data with a three series RC circuits as shown in the inset of Figure S8a. We found that, compared to device A (~180 Ω), device B has a relatively small charge exchange resistances R_{CE} (~50 Ω) at the same bias, indicating an efficient charge collection ability for $Cs_{0.05}(FA_{0.4}MA_{0.6})_{0.95}PbI_{2.8}Br_{0.2}$ based device. Furthermore, device B exhibits larger R_{rec} value than that of device A as shown in Figure S8c. This indicates that the interfacial recombination of device A is greater than that of device B, resulting in its lower V_{OC}. The IS result agrees well with the transient photovoltage decay measurements.

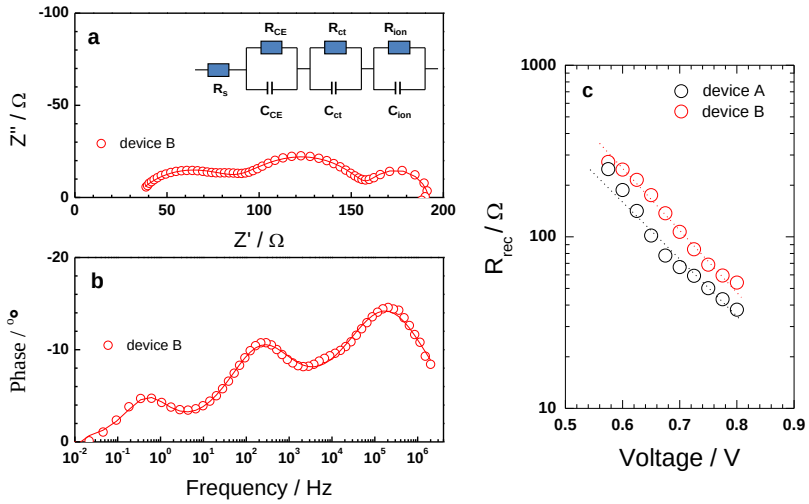

Figure S7. (a) Nyquist plot and (b) the corresponding Bode plot for the devices B measured in 100% LED light source with a bias at 0.75 V over frequency range from 10 mHz to 2 MHz. The solid lines are fitting results by using the equivalent circuit as shown in the inset. c) Interfacial recombination resistance (R_{rec}) for devices A and B.

Table S1. Photovoltaic parameters of perovskite solar cell for devices with MAI and FAI ratio of 4:1, 3:2, 2:3, 1:4 under AM 1.5 G simulated solar irradiation (100 mW cm^{-2}).

	V_{oc} [mV]	J_{sc} [mA cm^{-2}]	FF [%]	PCE [%]
MAI:FAI=4:1	920	14.56	59.97	7.75
MAI:FAI=3:2	900	16.00	67.67	9.73
MAI:FAI=2:3	852	17.23	62.77	9.23
MAI:FAI=1:4	846	17.50	60.63	8.96

Table S2. Photovoltaic parameters of perovskite solar cell for devices with PbI_2 and $PbBr_2$ ratio of 1:0, 9:1, 4:1, 3:2 under AM 1.5 G simulated solar irradiation (100 mW cm^{-2}).

	V_{oc} [mV]	J_{sc} [mA cm^{-2}]	FF [%]	PCE [%]
PbI_2:$PbBr_2$=1:0	909	14.20	64.72	8.35
PbI_2:$PbBr_2$=9:1	964	15.90	66.58	10.21
PbI_2:$PbBr_2$=4:1	974	13.54	66.02	8.71
PbI_2:$PbBr_2$=3:2	934	9.56	62.26	5.56

Table S3. List of Parameters for the absorption coefficient fitting as shown Figure S4.

	Eg[mV]	R_{ex}[meV]	σ_c[meV]	σ_{ex}[meV]
$FA_{0.4}MA_{0.6}PbI_{2.8}Br_{0.2}$	1.617	8.0	29.40	45.0
$Cs_{0.05}(FA_{0.4}MA_{0.6})_{0.95}PbI_{2.8}Br_{0.2}$	1.630	9.0	27.50	40.0
$Cs_{0.1}(FA_{0.4}MA_{0.6})_{0.9}PbI_{2.8}Br_{0.2}$	1.647	9.3	27.00	35.0
$Cs_{0.2}(FA_{0.4}MA_{0.6})_{0.8}PbI_{2.8}Br_{0.2}$	1.65	11.0	32.40	45.0

Table S4. Photovoltaic parameters of device B with different scan direction of reverse scan (RS) and forward scan (FS) under 100 mW cm^{-2} irradiation.

	V_{oc} [mV]	J_{sc} [mA cm^{-2}]	FF [%]	PCE [%]
Device B-FS	991	23.18	72.83	16.73
Device B-RS	1008	23.40	72.14	17.02

Table S5. Photovoltaic parameters of perovskite solar cell for devices A, B, C, and D under AM 1.5 G simulated solar irradiation (100 mW cm^{-2}).

	V_{oc} [mV]	J_{sc} [mA cm^{-2}]	FF [%]	PCE [%]
Device A	953	22.31	70.00	14.88
Device B	1008	23.40	72.14	17.02
Device C	903	17.63	66.37	10.57
Device D	889	12.61	68.07	7.64

Reference

1 J. Cui, F. Meng, H. Zhang, K. Cao, H. Yuan, Y. Cheng, F. Huang, M. Wang, *ACS Appl. Mater. Interface*, **2014**, *6*, 22862-22870.

2 G. E. Eperon, S. D. Stranks, C. Menelaou, M. B. Johnston, L. M. Herz, H. J. Snaith, *Energy Environ. Sci.*, **2014**, *7*, 982-988.

3 H. Li, K. Cao, J. Cui, S. Liu, X. Qiao, Y. Shen, M. Wang, *Nanoscale*, **2016**, *8*, 6379-6385.

4 G. Kieslich, S. Sun,AK Cheetham, *Chem. Sci.*, **2014**, *5*, 4712-4715.

5 S. Liu, K. Cao, H. Li, J. Song, J. Han, Y. Shen, M. Wang, *Solar energy*, **2017**, *144*, 158-165.

6 X. Xu, M. Wang, *Sci. China Chem.* **2017**, *60*, 396.